QO'QON DAVLAT PEDAGOGIKA INSTITUTI ILMIY XABARLARI
(2025-yil 3-son)

TABIIY FANLAR

NATURAL SCIENCES

18-CROWN-6 BASED SUPRAMOLECULAR STRUCTURE, HYDROGEN BONDING BEHAVIOUR AND ITS NONLINEAR OPTICAL PROPERTIES.

***Samandarov Elyorbek Shonazar ugli*[1]**
[1]*Khorezm Mamun branch of Uzbekistan Academy of Sciences*
E-mail: **samandarove6@gmail.com**

***Ibragimov Aziz Bakhtiyarovich*[2]**
[2]*Director of the Institute of General and Inorganic Chemistry of the Academy of Sciences*

***Yakubov Yuldosh Yusupboevich*[2]**
Institute of General and Inorganic Chemistry of Uzbekistan Academy of Sciences[2]

***C.Balakrishnan*[3]**
Department of Chemistry Erode Sengunthar Engineering College Erode, Tamil Nadu, India[3]

Abstract. The crystal structures of the host-guest supramolecular complexes [1,4,7,10,13,16-hexaoxacyclooctad ecane, pyridin-3-ylmethanaminium salt]·$2H_2O$ (I) and short form $[(P3MA)_2^{+}\cdot 2(18C6)]\cdot 2H_2O$ (18C6=18-crown-6(1,4,7,10,13,16-hexaoxacyclooctadecane); P3MA= pyridine-3-ylmethanamine were determined by single-crystal X-ray diffraction analysis. Supramolecular assembly is constructed via N–H•••O; O-H•••N interactions. Both complexes crystallize in the monoclinic system with the centrosymmetric space group Pn . The vibrational patterns in FT-IR spectra are used to identify functional groups. Direct band gap energies estimated by diffuse reflectance spectroscopy are 3.42 eV for (I) and 4.78 eV for (II). Molecular interactions are analyzed using Hirshfeld surfaces derived from single-crystal XRD data. Fingerprint plots of Hirshfeld surfaces were employed to quantify and analyze the percentage contributions of hydrogen bonding interactions. Crystal size -0.14x0.12x 0.11 mm^3

A Z-scan study was conducted to determine the third-order nonlinear optical (NLO) response.

Keywords.pyridin-3-ylmethanamine;1,4,7,10,13,16-hexaoxacyclooctadecane; 1,4,7,10,13,16-hexaox acyclooctadecane, pyridin-3-ylmethanaminium salt; hydrogen bond; crystal data; FT-IR spectroscopy.

Introduction. Crown ethers are pivotal in supramolecular and coordination chemistry due to their ability to form host-guest complexes with unique structures and diverse bonding interactions[1-3]. Ammonium-crown ether-based organic-inorganic assemblies have been extensively studied [4-5], where the stability of these complexes depends on the crown ether size and the nature of the protonated ammonium cation (e.g., NH_4^+, RNH_3^+). A key structural feature is the encapsulation of the $–NH_3^+$ group within the crown ether cavity [6-7]. Supramolecular networks arise from weak intermolecular interactions, including hydrogen bonds, charge transfer, and van der Waals forces[8]. These materials find applications in data storage, capacitors, sensors, and optical devices [9-11]. Third-order nonlinear optical properties of the crystal ere examined by the Z-scan technique. Hirshfeld surface analysis was used to quantify intra- and intermolecular interactions[12].

Experimental.

Synthesis and crystal growth.

18-Crown-6 (18C6) and pyridin-3-ylmethanamine (P3MA) were procured from Sigma Aldrich (Assay:

99%), while commercially available solvents from Merck were used without further purification. In a solvent system consisting of diethyl ether (5 mL) and methanol (10 mL) in a 1:2 (v/v) ratio, 18C6 (1.32 g, 5mmol) and pyridin-3-ylmethanamine (P3MA) (1.08 g, 10 mmol) were combined in a stoichiometric ratio of 1:2. The resulting mixture underwent reflux at 95-100 °C for 4 h (Scheme 1). Maintained in a constant temperature thermostat at 40 °C, crystallization occurred over 25–27 days, yielding crystals with dimensions of 1 × 2 × 1 mm³ (Yield: 80%). *(Scheme-1).*

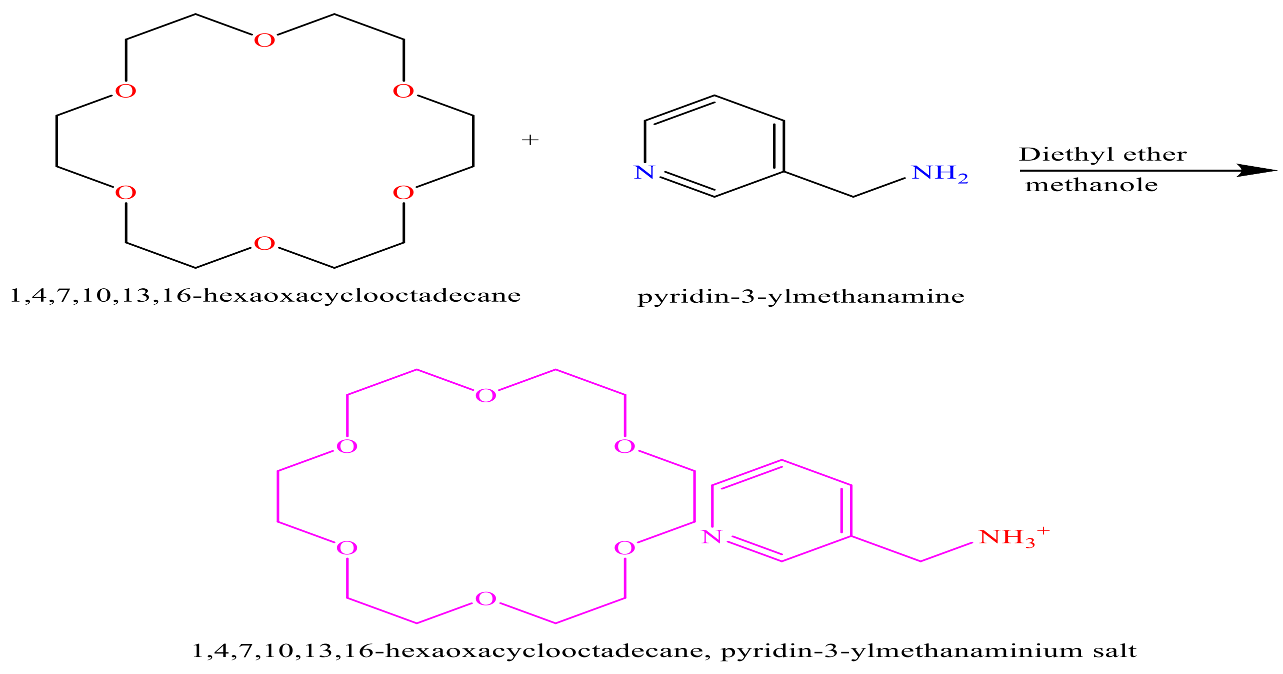

(Scheme-1). Synthesis of 18-Crown-6, pyridin-3-ylmethanaminium salt.

Single crystal X-ray structure analysis.

The crystal structure was elucidated by single-crystal XRD analysis. Crystallographic data and details of

the refinement parameters are listed in Table-1.

Information of plane spacing for monoclinic structure crystal systems.

$$\frac{1}{d^2} = \frac{1}{sin^2\beta} \cdot (\frac{h^2}{a^2} + \frac{k^2\, sin^2\beta}{b^2} + \frac{l^2}{c^2} - \frac{2hl\cos\beta}{ac})$$

The selected hydrogen bonds, bond distances and bond angles are listed in Tables 2-4. The ORTEP and packing diagram of 18C6•2(P3MA)•2(H_2O) are given in Fig-1. It crystallizes in the monoclinic system with centric space group Pn with Z = 2. The asymmetric unit consists of half 18C6, electron density peak is found near heavy atom iodine. Crystal is a layered type that cannot be separated. This caused bad data quality and high wR_2 value.Most of the amine/ammonium (R-NH_2, R-NH_3^+, etc.) containing crown ether complexes form N─H•••O/N-H•••O type of hydrogen bonds [15–17]. In the present study, the hydrogen bonds are only

OW─H•••O18C6 because of the inclusion of water molecules in the crown ether cavity. There is no contact between the -NH_2 group and oxygen atoms in 18C6 because -NH_2 groups form the intramolecular

hydrogen bonds.

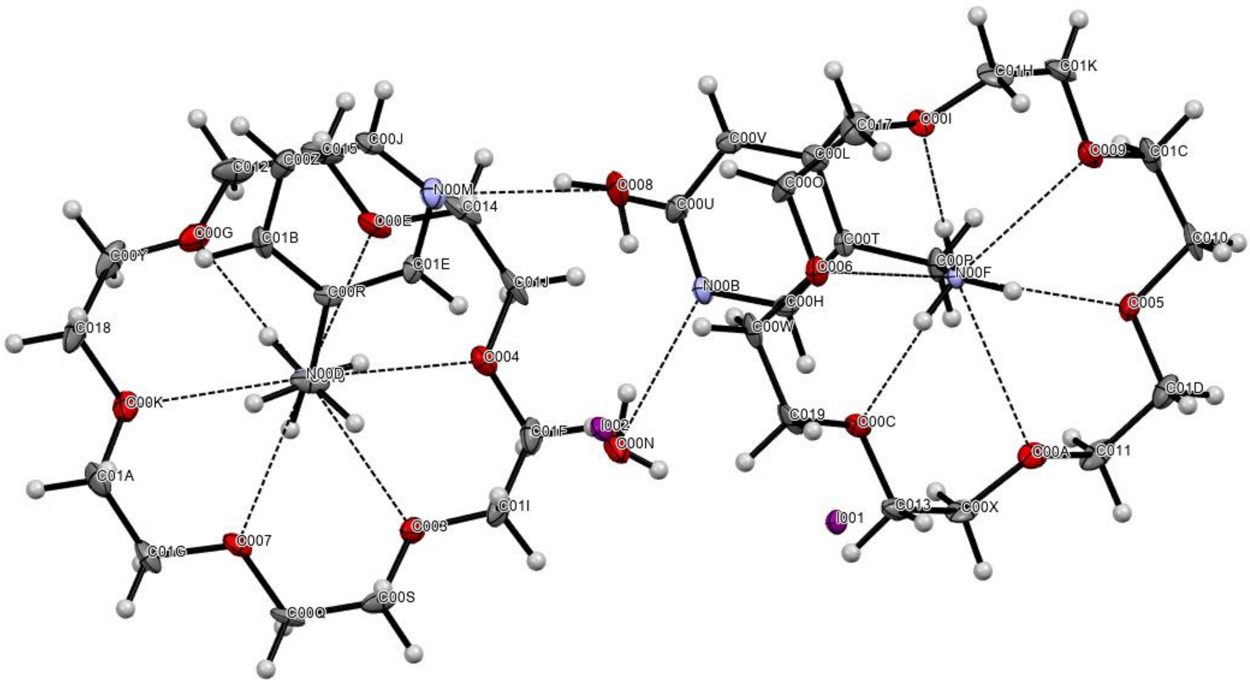

Fig-1. *(a) ORTEP drawing of the intermolecular H-bonds and (b) Nonlinear optical (NLO) materials.*

1,4,7,10,13,16-hexaoxacyclooctadecane, pyridin-3-ylmethanaminium salt.

molecule. Thermal ellipsoids are drawn with the 50% probability level.

Table -1. Crystal data and structure refinement for $[(P3MA)_2^{+}\cdot 2(18C6)]\cdot 2H_2O$.

Identification code	exp_393_CB08_auto
Empirical formula	$C_{36}H_{68}I_2N_4O_{14}$
Formula weight	1034.74
Temperature/K	107(5)
Crystal system	Monoclinic
Space group	Pn
a/Å	12.70250(10)
b/Å	9.45940(10)
c/Å	19.25390(10)
α/°	90
β/°	92.3510(10)
γ/°	90
Volume/Å^3	2311.56(3)
Z	2
ρ_{calc}g/cm^3	1.487
μ/mm^{-1}	11.216
F(000)	1060.0
Crystal size/mm^3	0.14 × 0.12 × 0.11
Radiation	Cu Kα (λ = 1.54184)
2Θ range for data collection/°	4.594 to 143.192
Index ranges	-15 ≤ h ≤ 15, -11 ≤ k ≤ 11, -23 ≤ l ≤ 23
Reflections collected	45306
Independent reflections	8957 [R_{int} = 0.0551, R_{sigma} = 0.0348]
Data/restraints/parameters	8957/2/520
Goodness-of-fit on F^2	1.040
Final R indexes [I>=2σ (I)]	R_1 = 0.0299, wR_2 = 0.0788
Final R indexes [all data]	R_1 = 0.0299, wR_2 = 0.0788
Largest diff. peak/hole / e Å^{-3}	1.36/-1.55
Flack parameter	0.000

Table-2.Hydrogen bonds for $[(P3MA)_2^{+}\cdot 2(18C6)]\cdot 2H_2O$. (A^0); R = 0.03.

D-H•••A	d(D-H)	d(H•••A)	<DHA	d(D•••A)	Symmetry
O(008) – H(00Y) •••N(00M)	0.8700	2.0200	2.866(6)	164.00	
N(00D) – H(00S) ••• O(003)	0.9100	2.5100	2.994(5)	114.00	
N(00D) – H(00S)••• O(007)	0.9100	2.0000	2.817(5)	149.00	
N(00D) – H(00S)••• O(00K)	0.9100	2.6000	2.918(5)	101.00	
N(00D) – H(00T) •••O(004)	0.9100	1.9900	2.876(6)	165.00	
N(00D) –H(00T) •••O(00E)	0.9100	2.4100	2.934(5)	117.00	
N(00D) – H(00W)•••O(00G)	0.9100	1.9900	2.892(5)	174.00	
N(00D) – H(00W)••• O(00K)	0.9100	2.5000	2.918(5)	109.00	

N(00F) – H(00K) •••O(006)	0.9100	2.4900	2.959(5)	113.00	
N(00F) –H(00K)••• O(00C)	0.9100	1.9500	2.849(5)	169.00	
N(00F) – H(00L)••• O(009)	0.9100	2.5500	2.898(5)	103.00	
N(00F)–H(00L)•••O(00I)	0.9100	2.0000	2.906(5)	177.00	
N(00F)–H(00M) •••O(005)	0.9100	2.0100	2.828(5)	149.00	
N(00F)–H(00M) ••• O(009)	0.9100	2.4900	2.898(5)	107.00	
N(00F)–H(00M)•••O(00A)	0.9100	2.5800	3.012(5)	109.00	
O(00N)– H(G) •••N(00B)	0.87(8)	2.11(8)	2.914(6)	154(8)	**1/2+x,1-y,1/2+z**

Table-3. Bond Distances $[(P3MA)_2^{+}\cdot 2(18C6)]\cdot 2H_2O$ (A^0). R = 0.03

Bond	Distances	Bond	Distances
O(007) –C(00Q)	1.416(7)	O(00N)–H(G)	0.87(8)
O(007) –C(01G)	1.440(7)	O(00N)–H(00)	0.77(8)
O(00E)–C(014)	1.428(7)	N(00D)–C(016)	1.499(6)
O(00E)–C(015)	1.412(8)	N(00M) –C(01E)	1.340(7)
O(00G) –C(00Y)	1.429(7)	N(00M)–C(00J)	1.331(8)
O(005)–C(01D)	1.435(7)	C(00Q) –C(00S)	1.489(8)
O(005)–C(010)	1.438(7)	C(00Y)–C(018)	1.507(8)
O(006)–C(00W)	1.424(7)	C(012)–C(015)	1.501(8)
O(006)–C(00O)	1.403(7)	C(014)–C(01J)	1.489(9)
C(01J) –H(01R)	0.9900	C(01K)–H(3)	0.9500
C(010)–C(01C)	1.497(9)	C(00P)–C(00T)	1.503(7)

Table-4.Bond Angles. (A^0). R = 0.03

Bond	Bond Angles	Bond	Bond Angles
C(00P) –N(00F)–H(00L)	109.00	H(00A) –C(00Q) –H(00B)	108.00
C(00P)–N(00F)–H(00M)	109.00	H(00C) –C(00S) –H(00D)	108.00
C(00Y)–C(018)–H(01G)	110.00	O(00A) –C(00X) –C(013)	108.9(5)
H(01I)–C(01A)–H(01J)	108.00	O(005) –C(010) –C(01C)	109.3(5)
O(00C)–C(013)–H(01X)	110.00	O(009) –C(01K) –H(3)	126.00
H(01W)–C(013)–H(01X)	108.00	N(00B) –C(00H) –C(00T)	123.5(4)
O(00I)–C(017)–H(B)	110.00	C(00T) –C(00L) –C(00V)	118.5(5)
N(00F)–C(00P)–C(00T)	112.9(4)	C(016)–C(00R) –C(01B)	121.3(5)
C(00H)–C(00T)–C(00P)	120.6(4)	C(016) –C(00R) –C(01E)	120.3(4)
C(00L)–C(00T)–C(00P)	121.1(4)	C(01B) –C(00R) –C(01E)	118.4(5)
C(00H) –C(00T) –C(00L)	118.2(4)	C(00J) –C(00Z) –C(01B)	118.2(5)
N(00B)–C(00U)–C(00V)	123.5(5)	N(00D) –C(016) –C(00R)	112.5(4)
C(00L)–C(00V)–C(00U)	119.3(5)	C(00R) –C(01B) –C(00Z)	118.9(5)
N(00B) –C(00H) –H(00N)	118.00	N(00M) –C(01E)–C(00R)	122.9(5)
C(00T) –C(00H) –H(00N)	118.00	C(00Z) –C(00J) –H(00X)	118.00

The percent elemental composition of compound 1,4,7,10,13,16-hexaoxacyclooctadecane, pyridin-3-ylmethanaminium salt was determined using a Thermo Scientific FlashSmart (CHNS/O) elemental analyzer. This analysis was performed by gas chromatographic separation of combustion gases based on the modified Dumas method.In order to assess the accuracy of the measurements, the results obtained from the analysis were compared in practical and theoretical terms.Table-5.

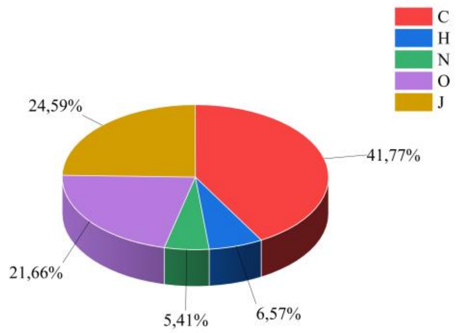

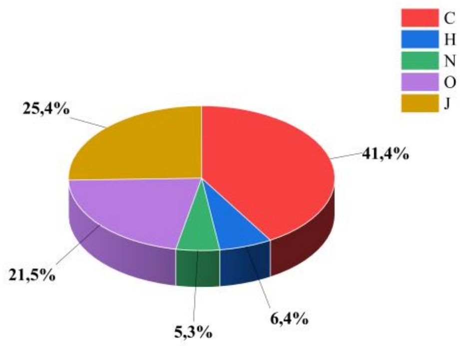

Table-5.

Compound	Mr	Compared	C %	H %	N %	O %
$C_{36}H_{68}I_2N_4O_{14}$	1034.12 gr/mole	Theoretical	41.77	6.57	5.41	21.66
		Practical	41.39	6.42	5.29	21.46

FT-IR spectroscopy. The characteristics vibrational spectra of (I)-(V) are shown in Table-6.

To interpret the FT-IR spectrum of 1,4,7,10,13,16-hexaoxacyclooctadecane, pyridin-3-ylmethanaminium salt , we will assign each peak based on the structure and functional groups present in the compound. Below is a detailed analysis of the peaks you provided.Table-6.

Peak (cm^{-1})	Assigment	Functional group
3147	N-H stretching	$-CH_2-NH_3^+$ (protonated methanaminium group)
3005	Aromatic C-H stretching	Pyridine ring
1575	Aromatic C=C stretching or N-H bending	Pyridine ring or $-CH_2-NH_3^+$
1464	Aromatic C-C stretching or N-H bending	Pyridine ring or $-CH_2-NH_3^+$
1425	Aromatic ring deformation or C-H bending	Pyridine ring
1387	Symmetric C-H bending	$-CH_2-$ group
1161	Ether C-O stretching	Crown ether (-C-O-C-)
1031	Ether C-O stretching	Crown ether (-C-O-C-)

762	Out-of-plane C-H bending	Pyridine ring
410	Metal-ligand interaction or ring deformation	Crown ether or pyridine ring

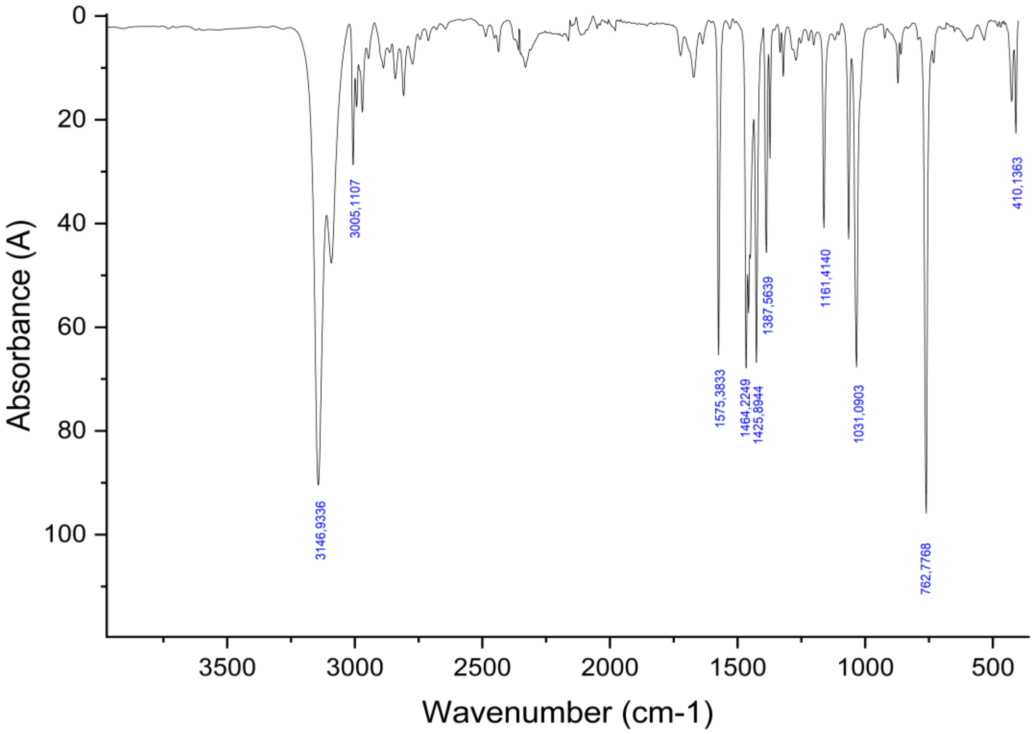

FT-IR spectroscopy-1,4,7,10,13,16-hexaoxacyclooctadecane, pyridin-3-ylmethanaminium salt.

Z-scan studies.

The nonlinear absorption, nonlinear refractive index, and third-order nonlinear susceptibility were determined by standard equations . The NLO properties of the cocrystal were experimentally determined by the Z-scan technique. Here, the open and closed aperture Z-scan curves are used for nonlinear absorption and nonlinear refractive index measurements. The transmittance intensity variations corresponding to the z values, and the closed and open aperture z-scan curves are represented.

REFERENCES.

1. Balakrishnan C. et al. Crystal structure and third-order nonlinear optical properties of supramolecular cocrystals of 18-crown-6 with 5-aminoisophthalic acid //Journal of Materials Science: Materials in Electronics. – 2024. – T. 35. – №. 8. – C. 614.
2. Chellakarungu B. et al. 18-Crown-6 based supramolecular structure, hydrogen bonding behaviour and its nonlinear optical properties. – 2023.

3. Guo M., Zhao M. M. 4-Bromoanilinium perchlorate 18-crown-6 clathrate //Structure Reports. – 2010. – T. 66. – №. 11. – C. o2836-o2836.
4. Vaganova T. A. et al. Polyhalogenated aminobenzonitriles vs. their co-crystals with 18-crown-6: amino group position as a tool to control crystal packing and solid-state fluorescence //CrystEngComm. – 2022. – T. 24. – №. 5. – C. 987-1001.
5. Wahan S. K., Bhargava G., Chawla P. A. Role of crown ethers as mediator in various chemical reactions //Ionic Liquids, Deep Eutectic Solvents, Crown Ethers, Fluorinated Solvents, Glycols and Glycerol. – 2023. – C. 145.
6. Merzlyakova E. et al. 18-Crown-6 coordinated metal halides with bright luminescence and nonlinear optical effects //Journal of the American Chemical Society. – 2021. – T. 143. – №. 2. – C. 798-804.
7. Shishkanova T. V. et al. Electrochemical sensor for phenylpropanolamine based on oligomer derived from 3-hydroxybenzoic acid with dibenzo-18-crown-6 //Journal of Electroanalytical Chemistry. – 2021. – T. 882. – C. 114963.
8. Bujor A. et al. Synthesis and Structural Analysis of a Nitrobenzofurazan Derivative of Dibenzo-18-Crown-6 Ether //Chemistry. – 2022. – T. 4. – №. 4. – C. 1696-1701.
9. Guezane-Lakoud S. et al. 2-Hydroxymethyl-18-crown-6 as an efficient organocatalyst for α-aminophosphonates synthesized under eco-friendly conditions, DFT, molecular docking and ADME/T studies //Journal of Biomolecular Structure and Dynamics. – 2024. – T. 42. – №. 7. – C. 3332-3348.
10. Tzeng B. C. et al. Luminescent Pt (II) complexes containing (1-aza-15-crown-5) dithiocarbamate and (1-aza-18-crown-6) dithiocarbamate: mechanochromic and solvent-induced luminescence //Inorganic Chemistry. – 2022. – T. 62. – №. 2. – C. 916-929.
11. Balakrishnan C., Vinitha G., Meenakshisundaram S. P. Novel C-H•••O hydrogen-bonded supramolecular complexes of 18-crown-6 with 1-alkylpyridinium iodide and its amino derivatives: Third-order nonlinear optical properties and Hirshfeld surface analysis //Journal of Molecular Structure. – 2022. – T. 1253. – C. 132310.
12. Adhami A. et al. Extraction of metal ions from water using a novel liquid membrane containing ZIF-8 nanoparticles, an ionic liquid, and benzo-18-crown-6 //Environmental Science: Water Research & Technology. – 2025.
13. Wineinger H. B. et al. Coordination Chemistry and Photoluminescence of Sm (II) Dibenzo-24-crown-8 Complexes //Inorganic Chemistry. – 2025.
14. Liu Y. et al. Esterified phenylalanine supramolecular motion: Anion order–disorder rotation induced reversible phase transition and dielectric-ferroelectric properties //Journal of Molecular Structure. – 2025. – T. 1328. – C. 141283.